Bandwidth Characterization of c-Si Solar Cells as VLC Receiver under Colored LEDs

Zhou, Yilong; Ibrahim, Aya ; Muttillo, Mirco; Manganiello, Patrizio; Ziar, Hesan; Isabella, Olindo

DOI
10.23919/SpliTech58164.2023.10193624

Publication date
2023

Document Version
Final published version

Published in
Proceedings of the 2023 8th International Conference on Smart and Sustainable Technologies (SpliTech)

Bandwidth Characterization of c-Si Solar Cells as VLC Receiver under Colored LEDs

Yilong Zhou
Photovoltaic Materials and Devices (PVMD) Group
Delft University of Technology
Delft, the Netherlands
Y.Zhou-15@tudelft.nl

Aya Ibrahim
Photovoltaic Materials and Devices (PVMD) Group
Delft University of Technology
Delft, the Netherlands
A.Ibrahim-14@student.tudelft.nl

Mirco Muttillo
Photovoltaic Materials and Devices (PVMD) Group
Delft University of Technology
Delft, the Netherlands
M.Muttillo@tudelft.nl

Patrizio Manganiello
Photovoltaic Materials and Devices (PVMD) Group
Delft University of Technology
Delft, the Netherlands
P.Manganiello@tudelft.nl

Hesan Ziar
Photovoltaic Materials and Devices (PVMD) Group
Delft University of Technology
Delft, the Netherlands
H.Ziar@tudelft.nl

Olindo Isabella
Photovoltaic Materials and Devices (PVMD) Group
Delft University of Technology
Delft, the Netherlands
O.Isabella@tudelft.nl

***Abstract*—This paper presents the fundamental study on the relationship between LED light sources and the performance of solar cell as receivers in visible light communication (VLC) links. Here, different colors of LEDs are modulated with a sinusoidal signal, and the bandwidth of the VLC system based on various c-Si PV architectures is characterized at different bias voltages. The preliminary results show that the bandwidth of such VLC system is highly influenced by the bias voltage, where higher bias voltage leads to lower bandwidth. This means that there is a trade-off between energy harvesting and communication performance when solar cells are used as VLC receivers. Meanwhile, we also observed that the bandwidth decreases as the LED irradiance level increases, and the color of LED (currently red and blue LEDs are characterized) does not pose a significant impact on the bandwidth. The highest bandwidth is found at 50 kHz for a VLC system using a 6-in TOPCON solar cell under 100 W/m^2 with 100 mV bias voltage.**

***Keywords*—Visible Light Communication (VLC), solar cells, LED colors, Photovoltatronics.**

I. Introduction

The fast development of wireless technology is demanding an increasing spectrum resource. The congested radio frequency (RF) spectrum has driven researchers to look for alternatives where Visible Light Communication (VLC) appears to be a promising technology. It complements the current wireless communication system by offering additional communication channels within the visible light spectrum range. A classic VLC system is comprised of a light source, Light Emitting Diode (LED) or LASER, and a photodiode (PD) as transmitter and receiver, respectively. The intensity of the transmitter is modulated at a high frequency for data transmission, and it varies the output current of the PD upon incidence which is further translated into voltage signals with a trans-impedance amplifier for decoding. This frequency is usually higher than the flicker fusion threshold, meaning that it is not perceivable by human eyes. Furthermore, using LED as a transmitter can still fulfill its primary lighting function [1].

Compared to traditional RF communication, VLC is advantageous in the following aspects:

- As a communication medium, visible light is unlicensed, so that it is freely available for broad development to alleviate the RF spectrum traffic.
- Visible light has a significantly wider bandwidth due to its higher frequency than radio waves, which permits broadband communication.
- Visible light cannot penetrate walls. Therefore, it prevents eavesdropping and enables high-security communication.
- LEDs are dominating the current lighting infrastructure, which can facilitate low-cost VLC deployment.
- LEDs consume little energy, and their long lifespan and high reliability ensure a low maintenance cost.

On the other hand, the wide deployment of VLC still sees a few challenges and one of the major limitations is attributed to the intrinsic drawback of using PDs as receivers. Despite their fast response time and high bandwidth, the communication performance of PDs degrades drastically under the exposure of ambient light ($>$200 W/m^2) which restrains its outdoor application [2]. Meanwhile, the operation of PDs requires an external power supply.

Photovoltaic (PV) cells can be a good candidate to bridge the gap between simultaneous energy harvesting and data transmission. They are primarily designed and optimized for the outdoor environment, and the produced energy can be used to power the entire communication system. Some studies have already demonstrated the potential of implementing PV cells as optical receivers in VLC systems [3]–[5]. In [4], a self-powered VLC setup manages to reach an error-free data

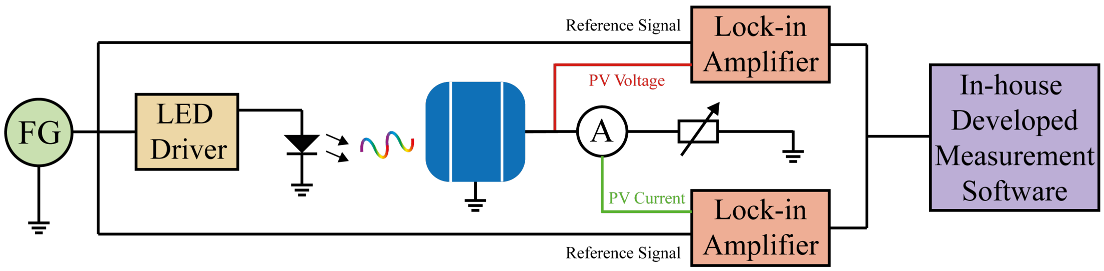

Fig. 1. Diagram of the experimental setup for bandwidth measurement of different c-Si PV architectures under colored LEDs. FG stands for function generator. The bias circuit is represented by a variable resistor for simplification. This bias circuit sets the operating point of the solar laminate and imposes a resistive load R_L in the AC circuit system.

TABLE I
KEY PARAMETERS OF THE C-SI PV ARCHITECTURES UNDER STANDARD TEST CONDITIONS (STC).

Solar Laminate	V_{oc} [mV]	I_{sc} [mA]	V_{mpp} [mV]	I_{mpp} [mA]	P_{mpp} [mW]	Area [cm^2]
Al-BSF (6-inch)	641.3	9443.6	521.4	8909.0	4646.0	244.3
Al-BSF (5-inch)	637.6	5955.3	506.2	5510.0	2789.0	153.0
Al-BSF-BF (6-inch)	643.2	9443.1	505.8	8857.0	4480.0	244.3
IBC (5-inch)	680.7	6464.0	566.1	5982.0	3387.0	153.0
PERC (6-inch)	688.1	4936.3	586.6	4710.0	2763.0	126.0
SHJ (6-inch)	743.0	8921.4	635.8	8499.0	5404.0	244.3
TOPCON (6-inch)	694.7	4908.7	588.6	4653.0	2738.0	126.0

rate of 8 kb/s with signal conditioning, and in [5], a data rate of 7 Mb/s is achieved with orthogonal frequency-division multiplexing (OFDM) under 3.5 W/m^2 of average irradiance. By adding an additional receiver circuit to apply a reverse bias to the solar panel with its own harvested energy, WH Shin et al. report an improved data transmission (17 Mbps with discrete multitone transmission (DMT)) and solar energy conversion [6]. Other researchers investigated different PV technologies where a-Si is used for weak light detection (down to 10 mW/m^2) and a data rate of 1 Mb/s OFDM signal can be successfully transmitted [7]. The impact of sunlight on the communication performance of a polycrystalline Si solar panel is also reported, and an increased irradiance leads to a lower data rate with a 940 nm laser transmitter [8].

While most of the studies have focused on improving the data rate, there is no research work to our knowledge which characterizes the fundamental interaction between the light source color and different solar cell architectures in the context of VLC. Therefore, the objective of this study is to investigate how different colors of LED light within visible light spectrum will influence the communication performance of solar cell as VLC receivers. In this article, c-Si solar cells are examined due to their dominating position in the PV industry. These encompass various architectures, including aluminum back surface field with (Al-BSF) and without busbars (Al-BSF-BF), passivated emitter rear contact (PERC), interdigitated back contact (IBC), silicon heterojunction (SHJ), and tunnel oxide passivated contact (TOPCON).

The rest of the paper is broken down into the following parts: Section II describes the experimental setup for bandwidth measurement of the VLC system using different c-Si PV architectures under different LED colors, each tested with 3 irradiance levels. Section III discusses the preliminary results, and a conclusion is drawn in Section IV.

II. EXPERIMENTAL SETUP

Figure 1 shows the block diagram of the experimental setup for bandwidth characterization of the VLC system with solar cells as receivers. The experiment is carried out for 5 c-Si PV architectures and 2 LED colors set at 3 different irradiance levels (100, 300 and 500 W/m^2). The solar cells are laminated before measurement (hereafter referred to as solar laminate) and all LEDs have a rated maximum power of 100 W. Table I and II list the most relevant parameters of the used solar laminates and LEDs, respectively.

TABLE II
LEDS AND THEIR WAVELENGTH AS CLAIMED BY THE MANUFACTURER.

LED	Wavelength [nm]
Blue	463
Red	623

A. Solar laminate I-V curve measurement

The *I-V* curve of the solar laminate is measured in 4-wire configuration with Keithley KickStart software and source meter (Keithley 2651A). LED light is fixed at 10 cm above the solar laminate, and by increasing its power, the desired irradiance level is achieved, assuming a linear relationship with the short-circuit current of solar laminate. A thermocouple is attached to the back of the solar laminate and the temperature is monitored with a Pico logger. When the temperature is stable, the *I-V* sweep is performed. The same procedure is repeated for each solar laminate under different LED colors and intensities. The DC parameters of a solar cell, such as series and shunt resistance, are extracted by fitting the *I-V* curve to a single-diode equivalent circuit model. The frequency sweep range for subsequent small-signal analysis is then determined using the open circuit voltage and maximum power point voltage obtained from the *I-V* curve. It is important to mention that the temperature effect is not taken into account in the analysis due to limitations in the setup.

B. Transmitter circuit

The transmitter circuit consists of an Agilent 33250A function generator (FG), several LEDs, and a custom-made LED driver. The setup uses the constant current (CC) method to drive the LED with the FG. Indeed, on top of the DC offset used to set the irradiance level, we superposed a small sinusoidal AC signal (V_{pp} = 5 mV) covering the frequency range from 25 to 250 kHz. All these components have relatively high bandwidth, thus, their contribution to the solar laminate bandwidth measurement is negligible.

The dynamic behavior of a solar cell can be modeled by a small-signal equivalent circuit as shown in Figure 2, where r_d is the dynamic resistance, C is the capacitance, R_p is the shunt resistance, and R_S is the series resistance of the solar cell. L represents the inductance due to the solar cell metallization and its interconnection with the load, and R_L is the load resistance.

C. Receiver Circuit

The receiver circuit includes the solar laminate, self-made bias circuit, two lock-in amplifiers (EG&G 7260 and EG&G 7225), and one multimeter (Keithley 2000). The measurement is automated by means of ad hoc in-house developed software. The bias circuit sets the operating point of the solar laminate. At every bias point, the frequency sweep is performed where the LED light is modulated with a small sinusoidal signal. In response to this, the *I-V* curve of the solar laminate changes, and it creates new intersections with the resistance line for both current and voltage, as exemplified in Figure 3. This tiny variation in the output is heavily buried in system noises. Therefore, lock-in amplifiers are used to pull out this small-signal AC information. The PV voltage is measured with a voltage probe that is directly connected to one of the lock-in amplifiers. The PV current is first converted to a voltage signal with a current probe (YOKOGAWA DLM5038) before entering the other lock-in amplifier. Here, the peak-to-peak signal at low frequency (25 Hz) is used as the reference S_{ref},

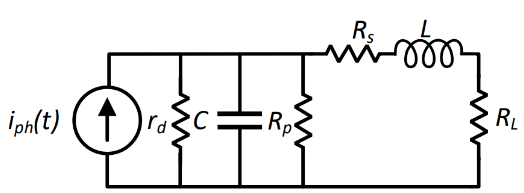

Fig. 2. Small-signal equivalent circuit model of a solar cell connected to a resistive load.

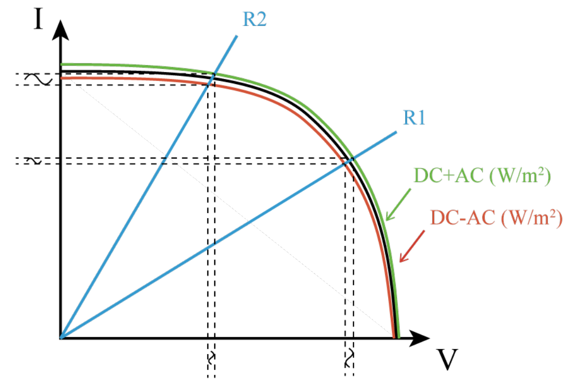

Fig. 3. Schematic representation of the response of the solar laminate upon receiving a modulated LED light signal. R1 and R2 represent two different load resistances. The *I-V* curve of the solar laminate changes marginally, which creates a new set of interactions for voltage and current.

and the signal gain at the different frequencies f is calculated with the equation below.

$$Gain(f) = 20log_{10}\frac{S_{out}(f)}{S_{ref}} \tag{1}$$

$S_{out}(f)$ is the peak-to-peak signal at each frequency f. The frequency at -3 dB gain is the bandwidth since the solar cell is a low-pass filter [9]. This frequency sweep is repeated for a few operating points from 100 mV to the open-circuit condition under different LED colors and intensities.

III. Preliminary Results

A. Bandwidth vs Bias Voltage

In Figure 4, the current and voltage bandwidth of the VLC system with solar laminates as receivers at various bias voltages are shown. In this case, the blue LED is used, and the irradiance level is set at 300 W/m^2. As the bias voltage increases, both the current and voltage bandwidth decrease. At the low bias voltage range, this decrease is marginal, while it ramps down exponentially at higher bias voltage. This is mostly due to the internal capacitance of the solar cells. At low bias voltage, the junction capacitance, which slightly changes in such a voltage range, dominates. At higher bias voltages instead, the diffusion capacitance, which changes exponentially with the bias voltage, becomes dominant [10]. This result indicates that higher power output is achieved at the expense of communication bandwidth. Therefore, a trade-off exists between energy harvesting and communication.

B. Current Bandwidth vs Irradiance Level

Figure 5 shows the change of current bandwidth of the VLC system based on 4 solar laminates at different bias voltages with the increase of irradiance. A blue LED is used in these experiments. As the irradiance increases, the current bandwidth reduces. This could be explained by the increased capacitance of the solar cell under higher irradiance for any given bias voltage, combined with a variation of the small-signal resistance of the device. Meanwhile, higher irradiance

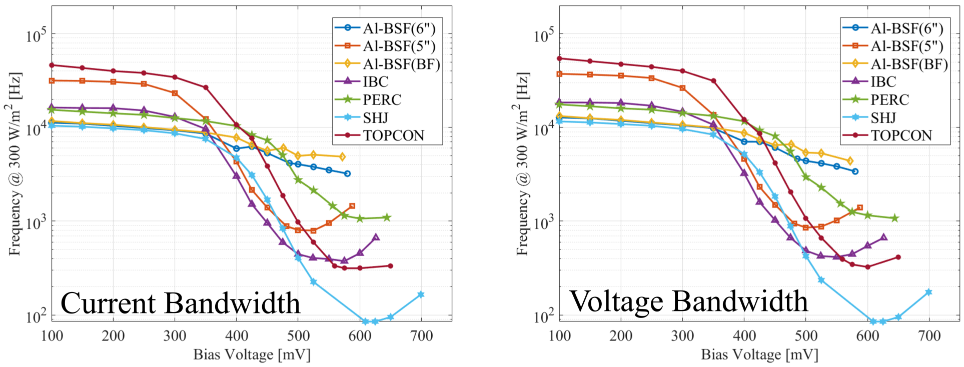

Fig. 4. Current and voltage bandwidth of the VLC system with different c-Si PV architectures at various bias voltages under 300 W/m^2 blue LED.

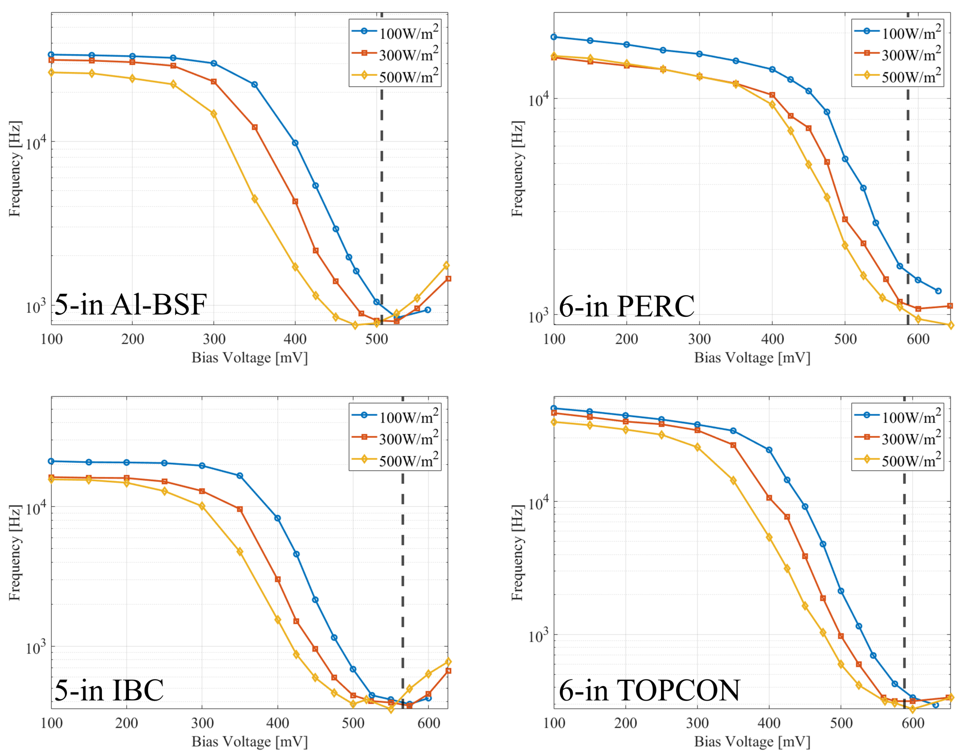

Fig. 5. Current bandwidth of the VLC system with 4 solar laminates versus different bias voltages at 3 irradiance levels of blue LED. The dashed line indicates the V_{mpp} at STC of each solar laminate.

results in a higher cell temperature which also contributes to the increase in capacitance [11]. On the other hand, we also observe an upward turn in the tail, indicating an increased bandwidth after maximum power point. This behavior could be attributed to the frequency-dependent nature of the capacitor, where the capacitance decreases as the frequency increases. This effect is more pronounced at higher static capacitance, which corresponds to the case of a higher bias voltage across the solar laminate [12].

C. Current Bandwidth vs LED Color

To study the effect of LED colors, we measured the bandwidth of the VLC system using different solar laminates at different bias voltages under red and blue lights of 300 W/m^2, and the results are shown in Figure 6. It can be observed that for c-Si PERC (6-in), IBC (5-in), SHJ (6-in), and Al-BSF-BF (6-in), using red light slightly increases the bandwidth ($\sim$12%) across the bias operating range. On the other hand, the difference on c-Si Al-BSF (5-in) and TOPCON (6-in) architectures is marginal, and the blue light performs better at low bias voltage range while red light outperforms above 300 mV. The reason behind still requires further investigation.

IV. Conclusion

In this paper, we investigate the dynamic performance of different c-Si solar cell architectures to be used as receivers

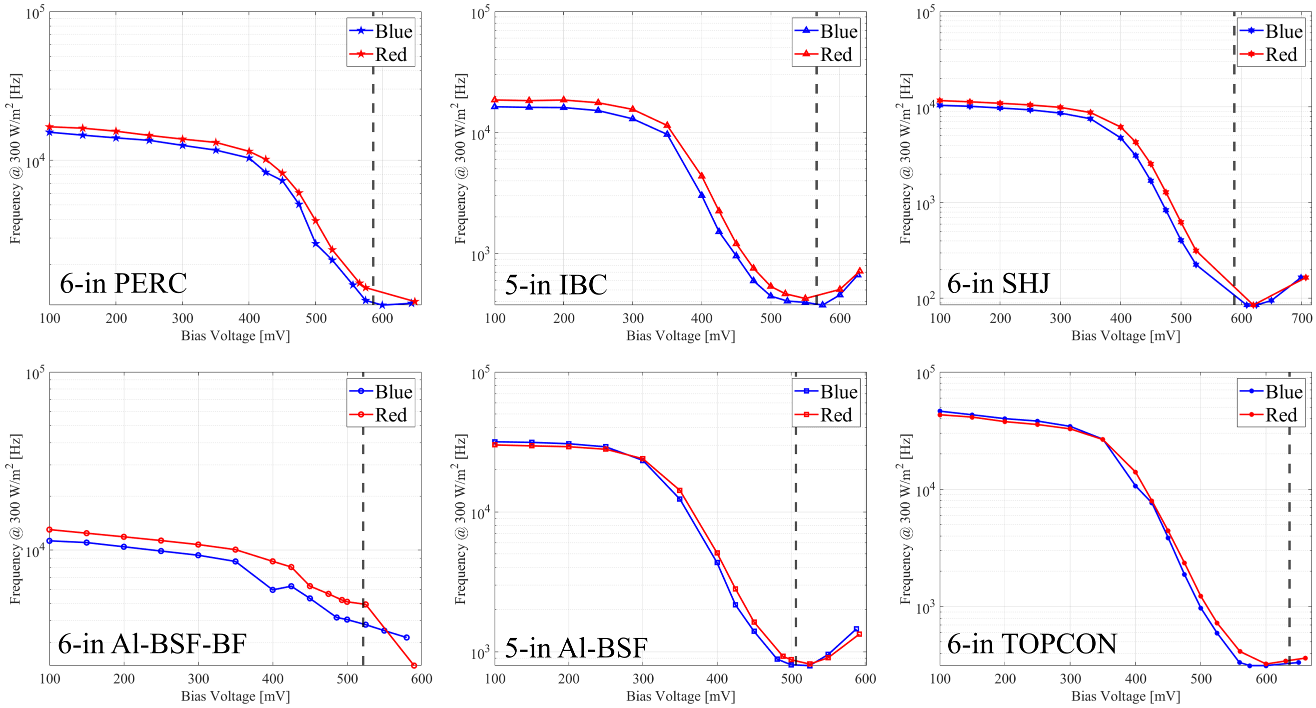

Fig. 6. Current bandwidth of the VLC system with various solar laminates under two different LED colors (red and blue) from 100 mV to open circuit condition. The dashed line indicates the V_{mpp} at STC of each solar laminate.

in VLC links by measuring their bandwidth at different bias voltages under red and blue LEDs. The result shows that the bandwidth is significantly influenced by the bias voltage at which the solar laminate is working, and a smaller bandwidth is reported as the bias voltage increases. This means that high bandwidth and maximum power production are competing, and a trade-off exists between communication performance and energy harvesting when using these types of solar laminates as VLC receivers. Meanwhile, we also observed that under higher LED luminance intensity, the bandwidth of VLC system decreases across the bias voltage range. Using different colors of LED does not show a big influence on the bandwidth, although slightly better performance is seen with red LED for c-Si PERC, IBC, SHJ and Al-BSF-BF architectures. Our future plan is to characterize the bandwidth of the c-Si solar-cell-based VLC system using LEDs of other colors within the visible light spectrum. Additionally, the signal-to-noise ratio and bit-rate error of such VLC system are also planned to be measured.

References

[1] Z. Wang, D. Tsonev, S. Videv, and H. Haas, “On the Design of a Solar-Panel Receiver for Optical Wireless Communications with Simultaneous Energy Harvesting,” *IEEE Journal on Selected Areas in Communications*, vol. 33, no. 8, pp. 1612–1623, 8 2015.

[2] N. Lorriere, N. Betrancourt, M. Pasquinelli, G. Chabriel, J. Barrere, L. Escoubas, J. L. Wu, V. Bermudez, C. M. Ruiz, and J. J. Simon, “Photovoltaic solar cells for outdoor lifi communications,” *Journal of Lightwave Technology*, vol. 38, no. 15, pp. 3822–3831, 2020.

[3] S. M. Kim and J. S. Won, “Simultaneous reception of visible light communication and optical energy using a solar cell receiver,” *International Conference on ICT Convergence*, pp. 896–897, 2013.

[4] B. Malik and X. Zhang, “Solar panel receiver system implementation for visible light communication,” *Proceedings of the IEEE International Conference on Electronics, Circuits, and Systems*, vol. 2016-March, pp. 502–503, 3 2016.

[5] Z. Wang, D. Tsonev, S. Videv, and H. Haas, “Towards self-powered solar panel receiver for optical wireless communication,” *2014 IEEE International Conference on Communications, ICC 2014*, pp. 3348–3353, 2014.

[6] S.-H. Yang, D.-H. Kwon, S.-K. Han, and W.-H. Shin, “Self-reverse-biased solar panel optical receiver for simultaneous visible light communication and energy harvesting,” *Optics Express, Vol. 24, Issue 22, pp. A1300-A1305*, vol. 24, no. 22, pp. A1300–A1305, 10 2016.

[7] M. Kong, M. Kong, J. Lin, J. Lin, C. H. Kang, C. Shen, Y. Guo, X. Sun, M. Sait, Y. Weng, H. Zhang, T. K. Ng, and B. S. Ooi, “Toward self-powered and reliable visible light communication using amorphous silicon thin-film solar cells,” *Optics Express, Vol. 27, Issue 24, pp. 34542-34551*, vol. 27, no. 24, pp. 34 542–34 551, 11 2019.

[8] S. Das, A. Sparks, E. Poves, S. Videv, J. Fakidis, and H. Haas, “Effect of Sunlight on Photovoltaics as Optical Wireless Communication Receivers,” *Journal of Lightwave Technology*, vol. 39, no. 19, pp. 6182–6190, 10 2021.

[9] D. van Nijen, P. Manganiello, M. Muttillo, M. Zeman, and O. Isabella, “Characterizing the Capacitance of Various Industrial Crystalline Silicon Solar Cells,” in *WCPEC-8*, 2022.

[10] M. Pravettoni, D. Poh, J. Prakash Singh, J. Wei Ho, and K. Nakayashiki, “The effect of capacitance on high-efficiency photovoltaic modules: A review of testing methods and related uncertainties,” *Journal of Physics D: Applied Physics*, vol. 54, no. 19, 5 2021.

[11] P. A. Cotfas, D. T. Cotfas, P. N. Borza, D. Sera, and R. Teodorescu, “Solar cell capacitance determination based on an RLC resonant circuit,” *Energies*, vol. 11, no. 3, 2 2018.

[12] O. Almora, Y. Zhao, X. Du, T. Heumueller, G. J. Matt, G. Garcia-Belmonte, and C. J. Brabec, “Light intensity modulated impedance spectroscopy (LIMIS) in all-solid-state solar cells at open-circuit,” *Nano Energy*, vol. 75, p. 104982, 9 2020.